**TELKOMNIKA Telecommunication, Computing, Electronics and Control**
Vol. 19, No. 2, April 2021, pp. 603~607
ISSN: 1693-6930, accredited First Grade by Kemenristekdikti, Decree No: 21/E/KPT/2018
DOI: 10.12928/TELKOMNIKA.v19i2.16855 

# Effects of $BaSO_4$ nano-particles on the enhancement of the optical performance of white LEDs

**Huu Phuc Dang[1], Phung Ton That[2], Dao Huy Tuan[3]**
[1]Faculty of Fundamental Science, Industrial University of Ho Chi Minh City, Vietnam
[2]Faculty of Electronics Technology, Industrial University of Ho Chi Minh City, Vietnam
[3]Faculty of Electrical and Electronics Engineering, Ton Duc Thang University, Ho Chi Minh City, Vietnam

**Article Info**

***Article history:***

Received Jun 2, 2020
Revised Oct 9, 2020
Accepted Oct 23, 2020

***Keywords:***

$BaSO_4$
Color uniformity
Luminous flux
Mie-scattering theory

**ABSTRACT**

The usage of $BaSO_4$ nanoparticles on WLEDs luminous flux and color uniformity improvements have been analyzed and demonstrated in this manuscript. The mixture of $BaSO_4$ and silicone placed on the yellow phosphor layer benefits the internal light scattering and thus enhances the angular correlated color temperature (CCT) homogeneity. Specifically, the blue-light intensity at large angles tend to increase and results in light intensity discrepancy, which can be corrected with added $BaSO_4$. In addition to this, the $BaSO_4$-silicone composite modifies the refractive index of the air-phosphor layer interface to an appropriate value, and thus, the luminous efficiency increases. The results show that the CCT deviations is reduced by 580 K, from 1000 K to 420 K, within the angle range from $-70^0$ to $+70^0$ with $BaSO_4$ in the phosphor structure. The increase in luminous flux is also recorded by 2.25%, in comparison with that of the non-$BaSO_4$ traditional structure, at the 120-mA driving current. Hence, integrating $BaSO_4$ nanoparticles into the remote phosphor structure can contributes to the enhancement of both lumen output and CCT uniformity.



***Corresponding Author:***

Dao Huy Tuan
Faculty of Electrical and Electronics Engineering
Ton Duc Thang University
No. 19 Nguyen Huu Tho Street, Tan Phong Ward, District 7, Ho Chi Minh City, Vietnam
Email: daohuytuan@tdtu.edu.vn

## 1. INTRODUCTION

High-power white light-emitting diodes (WLEDs) have been proposed as a potential lighting source for solid-state lighting (SSL) devices, which could replace the traditional one [1, 2]. Several techniques to manufacture WLEDs have been applied, yet the most popular one is dispersing yellow $Y_3Al_5O_{12}$ (YAG) phosphor on the blue LED chip. The LEDs fabricated by this method is called phosphor-converted white light-emitting diodes (pc-LEDs) [3-5]. The pc-LEDs can offer a high lighting efficiency and also a cost-saving production process, but they have not yielded good color uniformity and high light extraction at the air-phosphor layer interface. Meanwhile, enhancing the lumen efficiency of WLEDs by elevating the light extraction has been focused and researched extensively in recent studies [6-8]. Thus, researchers have come up with many packaging structures, for instances, using a hemi-spherically shaped encapsulation [9] and the ELiXIR pc-LEDs structure with internal reflection, to accomplish high light extraction [10]. However, the light loss still occurs in these structures, which reduce the overall efficiency of WLEDs [11, 12]. In particular, a considerable portion of yellow rays emitted from the yellow phosphor layer are scattered back to the LED chip and finally being absorbed. Researchers figured out that to avoid the backscattering effect, the solution is to address the re-absorption issue by providing a sufficient distance between the LED chip and the phosphor layer. Therefore, innovative structures were introduced to achieve this purpose, including the ring-remote structure and scattered photon extraction (SPE) [13-15].

According to the findings from previous articles, the remote phosphor structure is proved to have superior lumen efficacy to traditional dispersing design. However, throughout the duration of fabricating the remote phosphor structure, there is a problem related to the surface of the concave encapsulant, which is the phosphor thickness inhomogeneity [16-18]. Additionally, the angular-dependent blue light paths of this packaging design usually cause a non-uniform excitation, leading to the yellow ring phenomenon. Thus, we proposed to apply $BaSO_4$ nanoparticles to the remote packaging design of WLEDs as a solution for this issue. The purpose of using $BaSO_4$ material is to take advantage of its superior scattering ability to enhance the blue light intensity at large angles, from which the angular color correlated temperature (CCT) homogeneity is elevated [19-22]. In addition to this, the refractive index at the interface of the air and phosphor film is adjusted with the addition of $BaSO_4$, and thus, the luminous efficiency is also enhanced.

## 2. EXPERIMENT

The schematic diagrams of WLEDs are illustrated in Figure 1. The process of producing conventional remote phosphor structure is comprised of 3 main steps. Firstly, the blue LED chips are attached to the lead frame. Secondly, the transparent silicone glue is dispensed into the lead frame and cured at the temperature of 150 $^0$C within an hour. Thirdly, a slurry of phosphor suspension is created by the blending the phosphor powers, silicone binding agent, and alkyl-based solvent together. In addition, according to previous studied, the uniformity of the phosphor slurry can be improved by using the pulse spray coating method with an interval control. Afterwards, this slurry is placed onto the silicone surface to complete the remote structure which is presented in Figure 1 (a). The blue LED chips used in the experimented model are the 24-mile-square ones whose emission wavelengths peak at 450 nm. Additionally, each bare LED chip has 95 mW radiant flux at 120 mA driving current. The yellow phosphor $Y_3Al_5O_{12}$ (YAG) particle has a size of 12 µm.

The process of fabricating remote phosphor structure with $BaSO_4$ is similar to the traditional one, but $BaSO_4$ is used instead of the yellow phosphor to combine with the other two materials. The simulated of $BaSO_4$ remote phosphor packaging is shown in Figure 1 (b). Moreover, the $BaSO_4$ is added with the concentration of 5%. The input parameters of the LED chips in this structure is the same as those in the conventional one. Through the cross-sectional scanning electron microscopic (SEM) image, we can know that the particle size of $BaSO_4$ in the silicone encapsulant is approximately 300 nm. Besides, the energy dispersive spectrometer (EDS) is utilized to analyze the components of the encapsulant containing $BaSO_4$ and silicone.

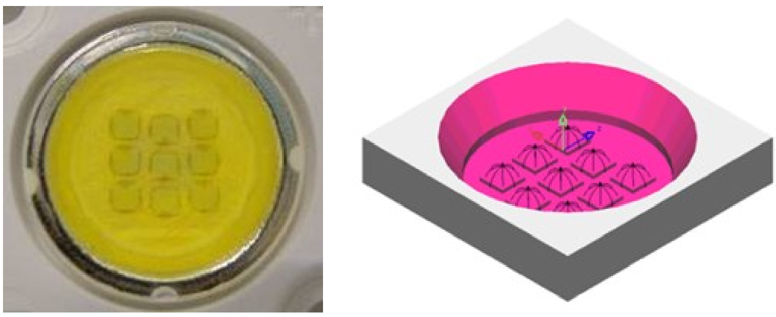

(a) (b)

Figure 1. (a) Photograph of WLEDs sample, (b) The simulated WLEDs model

## 3. RESULTS AND DISCUSSION

The general definition of the angular-dependent CCT homogeneity can be demonstrated as the following equation [23-25]:

Angular-dependent CCT uniformity = Max CCT – Min CCT

Figure 2 shows the changes of CCT deviations in connection with different particles weight of $BaSO_4$. As can be seen, the deviation of CCT reaches its lowest level when the weight of $BaSO_4$ is 10 mg cm$^{-2}$. The results present that this is the optimal weight for $BaSO_4$ to be applied as the CCT uniformity can be improved by 58%, or in other words, the CCT deviations reduce from 1000 K to 420 K in the angles from $-70^0$ to $70^0$, in comparison with that of the traditional structure. In the traditional packaging structure, the extraction of blue lights at large angles is inferior as they are trapped and reflected within the phosphor layer, and this phenomenon results in the inhomogeneous color mixing of blue and yellow rays. On the other hand, when added $BaSO_4$ the scattering events are improved, leading to a more uniform distribution of the blue and yellow lights. When the weight of $BaSO_4$ is more than 10 mg $cm^{-2}$, the CCT deviations are also affected. However, the structure with >10 mg $cm^{-2}$ still performs better than the conventional design.

In addition, the experiment outcomes indicate that the 10 mg $cm^{-2}$ $BaSO_4$ yields better luminous efficiency, as presented in Figure 3. At the driving current of 120 mA, the $BaSO_4$ structure can achieve 2.25% enhancement in luminous efficiency. Furthermore, the refractive index variation at the air-encapsulant interface is degraded, which probably increases the light extraction efficiency. As the $BaSO_4$-silicone film has the refractive index of 1.5, and the phosphor-silicone's is 1.8, the $BaSO_4$ will results in a sufficient gradient between air and the encapsulant layer.

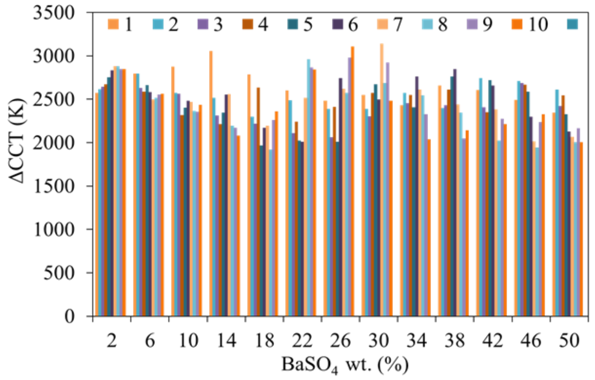


Figure 2. CCT deviations of BaSO4 particles with different diameters

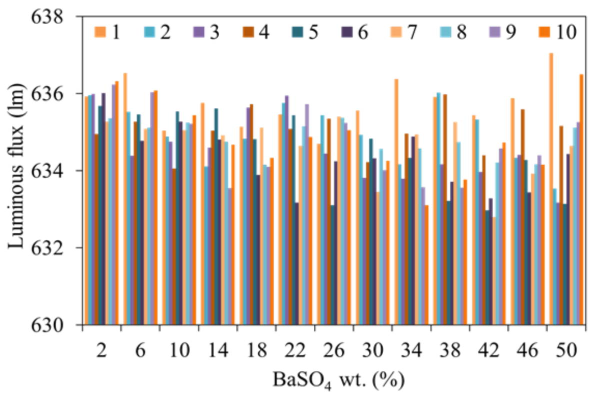


Figure 3. Luminous fluxes of BaSO4 particles with different diameters

To investigate more about $BaSO_4$ scattering ability in the visible range, the haze intensity is calculated by the two parameters: the total transmittance and the diffractive transmittance (non-specular transmittance), which can be expressed as [26]:

$$\text{Haze intensity} = T_{diffraction}/T_{total} \times 100\%$$

The diffractive and total transmittances are presented by $T_{diffraction}$ and $T_{total}$, respectively. Additionally, it is noted that the diffractive transmittance does not include the zero-order diffraction. The computed results demonstrated that the haze intensity of the non-$BaSO_4$ silicone layer stays at a low level which is around 0%. However, this parameter shows an upward trend when $BaSO_4$ appears in the silicone film, and tends to develop along with the increase in $BaSO_4$ particle weight. Moreover, the scattering is likely to be stronger as the haze intensity is higher. Besides, the better the scattering ability is, the more uniform the angular CCT becomes. Thus, $BaSO_4$ is a solution for the inhomogeneous CCT problem.

The changes of blue and yellow light scattering intensities in the normal direction with various $BaSO_4$ diameters are analyzed by using the full-field finite-difference time-domain (FDTD) simulation for the illustration of the impacts of $BaSO_4$ particle sizes on angular-dependent CCT and lumen efficacy. Given that $BaSO_4$-silicon layer's refractive index is 1.5, and $BaSO_4$ concentration is 5%, 400 nm turns out to be the most effective diameter of $BaSO_4$ as it can accomplish higher angular-dependent scattering intensity in the blue and yellow light (450 nm and 560 nm, respectively), compared to results of the other sizes. Though the color uniformity is obviously enhanced with the improvement in the light scattering, the blue and yellow light transmittance show some disadvantages. One of them is the increased absorption as the thickness of the $BaSO_4$-silicone layer grows, which will decrease the luminous performance. With $BaSO_4$ diameter at 300 nm, the absorbed light can make up 5-15% of the total amount, and this number tends to increase if the size of $BaSO_4$ becomes larger. Thus, the light absorption must be considered together with the light scattering when choosing the appropriate diameter for $BaSO_4$ nanoparticle so that WLED devices can achieve better CCT uniformity and light output power.

The influence that $BaSO_4$ has on the emission of the structure is investigated by the measurements of blue and yellow light angular-dependent relative intensity. It is reported that in $BaSO_4$ remote structure, the variety of blue light angles increases while the normal-direction blue light decreases in comparison to the conventional one. This implies the strong impacts of $BaSO_4$ scattering property on the light path of the blue photons that cause the increase of CCT deviation. Meanwhile, the light distribution of yellow rays in $BaSO_4$ remote phosphor structure is nearly the same as that in the conventional package. This phenomenon can be explained by the wavelength-dependent haze ratio of 10 mg $cm^{-2}$ $BaSO_4$ layer: its haze for yellow light with wavelength at about 600 nm is 30%, while for the ~ 450 nm blue rays is 35%. The higher haze percent results in the strong light scattered. Therefore, it can be said that the yellow-light scattering events are less than the blue-light ones, contributing to the lower CCT deviation as the blue and yellow lights are mixed more uniformly. Additionally, the haze measurement exhibits that the diffused component of 600 nm yellow light is half that of the 450 nm blue ray. Concluded from these findings, the CCT deviation has a close connection with the blue-light angle variations. Moreover, the blue-light relative intensity that is dependent on $BaSO_4$ weight was studied at the angle of $70^0$. The results reveal that 10 mg $cm^{-2}$ $BaSO_4$ is the most advantageous condition for the enhancement of WLEDs CCT uniformity as it exhibits the highest blue-light intensity at large angles.

## 4. CONCLUSION

The enhancement in CCT homogeneity and light output with the addition of $BaSO_4$ in the silicone layer is reported in this article. In particular, $BaSO_4$-silicone layer can get 58% improvement of CCT uniformity in comparison with the conventional design. Moreover, the presence of $BaSO_4$ helps to increase the lumen output by 2.25% at the driving current of 120 mA. The scattering effect of $BaSO_4$ is also analyzed through the haze intensity measurement. The outcomes reveal that the remote structure with 10 mg $cm^{-2}$ $BaSO_4$ can achieve the lowest angular CCT deviation level. In addition to this, the yellow ring phenomenon is likely eliminated without sacrificing the lighting output. Hence, manufacturers can use 10 mg $cm^{-2}$ $BaSO_4$ in the remote phosphor structure to accomplish high-quality WLED generation.

## REFERENCES

[1] H. S. E. Ghoroury, *et al.*, "Color temperature tunable white light based on monolithic color-tunable light emitting diodes," *Opt. Express,* vol. 28, pp. 1206-1215, 2020.
[2] H. Lee, *et al.*, "Phosphor-in-glass with Nd-doped glass for a white LED with a wide color gamut," *Opt. Lett*, vol. 43, pp. 627-630, 2018.
[3] Y. Tang, *et al.*, "Enhancement of luminous efficacy for LED lamps by introducing polyacrylonitrile electrospinning nanofiber film," *Opt. Express,* vol. 26, no. 21, pp. 27716-27725, 2018.
[4] W. Gao, *et al.*, "Color temperature tunable phosphor-coated white LEDs with excellent photometric and colorimetric performances," *Opt. Express,* vol. 57, pp. 9322-9327, 2018.
[5] S. K. Abeysekera, *et al.*, "Impact of circadian tuning on the illuminance and color uniformity of a multichannel luminaire with spatially optimized LED placement," *Opt. Express,* vol. 28, no. 1, pp. 130-145, 2020.
[6] L. Xiao, *et al.*, "Spectral optimization of phosphor-coated white LED for road lighting based on the mesopic limited luminous efficacy and IES color fidelity index," *Appl. Opt,* vol. 57, no. 4, pp. 931-936, 2018.
[7] L. Yang, *et al.*, "Thermally stable lead-free phosphor in glass enhancement performance of light emitting diodes application," *Appl. Opt,* vol. 58, no. 15, pp. 4099-4104, May 2019.
[8] L. Duan, *et al.*, "Wide color gamut display with white and emerald backlighting," *Appl. Opt,* vol. 57, pp. 1338-1344, 2018.

[9] S. Bindai, *et al.*, "Realization of phosphor-in-glass thin film on soda-lime silicate glass with low sintering temperature for high color rendering white LEDs," *Appl. Opt,* vol. 58, pp. 2372-2381, 2019.
[10] H. P. Huang, *et al.*, "White appearance of a tablet display under different ambient lighting conditions," *Opt. Express,* vol. 26, no. 4, pp. 5018-5030, 2018.
[11] A. Zhang, *et al.*, "Tunable white light emission of a large area film-forming macromolecular complex with a high color rendering index," *Opt. Mater. Express,* vol. 8, no. 12, pp. 3635-3652, Dec. 2018.
[12] W. Wang, *et al.*, "Red photoluminescent Eu3+-doped Y2O3 nanospheres for LED-phosphor applications: Synthesis and characterization," *Opt. Express,* vol. 26, no. 26, pp. 34820-34829, 2018.
[13] T. Han, *et al.*, "Spectral broadening of a single Ce3+-doped garnet by chemical unit cosubstitution for near ultraviolet LED," *Opt. Mater. Express,* vol. 8, pp. 3761-3769, 2018.
[14] A. Ullah, *et al.*, "Household light source for potent photo-dynamic antimicrobial effect and wound healing in an infective animal model," *Biomed. Opt. Express,* vol. 9, no. 3, pp. 1006-1019, Mar. 2018.
[15] H. Gu, *et al.*, "Design of two-dimensional diffractive optical elements for beam shaping of multicolor light-emitting diodes," *Appl. Opt,* vol. 57, pp. 2653-2658, 2018.
[16] Z. Li, *et al.*, "Effect of flip-chip height on the optical performance of conformal white-light-emitting diodes," *Opt. Lett*, vol. 43, pp. 1015-1018, 2018.
[17] L. Qin, *et al.*, "Luminance calculation method accounting for mesopic vision and fog penetration ability," *Appl. Opt,* vol. 59, pp. 683-686, 2020.
[18] G. Tan, *et al.*, "High dynamic range liquid crystal displays with a mini-LED backlight," *Opt. Express,* vol. 26, pp. 16572-16584, 2018.
[19] B. Jain, *et al.*, "High performance electron blocking layer-free InGaN/GaN nanowire white-light-emitting diodes," *Opt. Express*, vol. 28, pp. 665-675, 2020.
[20] L. Wu, *et al.*, "Hybrid warm-white organic light-emitting device based on tandem structure," *Opt. Express,* vol. 26, pp. A996-A1006, 2018.
[21] A. Ferrero, *et al.*, "Index for the evaluation of the general photometric performance of photometers," *Opt. Express,* vol. 26, pp. 18633-18643, 2018.
[22] C. Zhang, *et al.*, "All-inorganic silicon white light-emitting device with an external quantum efficiency of 1.0%," *Opt. Express*, vol. 28, pp. 194-204, 2020.
[23] Y. J. Park, *et al.*, "Development of high luminous efficacy red-emitting phosphor-in-glass for high-power LED lighting systems using our original low Tg and Ts glass," *Opt. Lett*, vol. 44, pp. 6057-6060, 2019.
[24] H. Yuce, *et al.*, "Phosphor-based white LED by various glassy particles: control over luminous efficiency," *Opt. Lett*, vol. 44, no.3, pp. 479-482, 2019.
[25] P. Kumar, *et al.*, "Enhanced exclusive-OR and quick response code-based image encryption through incoherent illumination," *Appl. Opt,* vol. 58, pp. 1408-1412, 2019.
[26] G. Xia, *et al.*, "Comparison of MAP method with classical methods for bandpass correction of white LED spectra," *Journal of the Opticcal Society of America A,* vol. 36, no. 5, pp. 751-758, 2019.